



Universiteit  
Leiden  
The Netherlands

## The two faces of MuSK antibody pathogenicity and their cause and consequences in myasthenia gravis

Vergoossen, D.L.E.

### Citation

Vergoossen, D. L. E. (2023, March 7). *The two faces of MuSK antibody pathogenicity and their cause and consequences in myasthenia gravis*. Retrieved from <https://hdl.handle.net/1887/3567889>

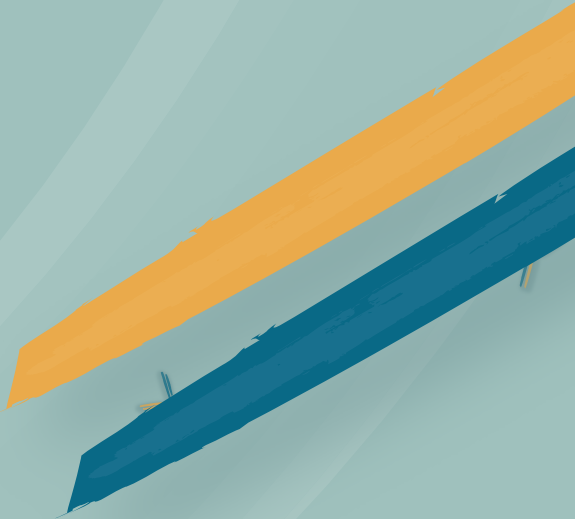
Version: Publisher's Version

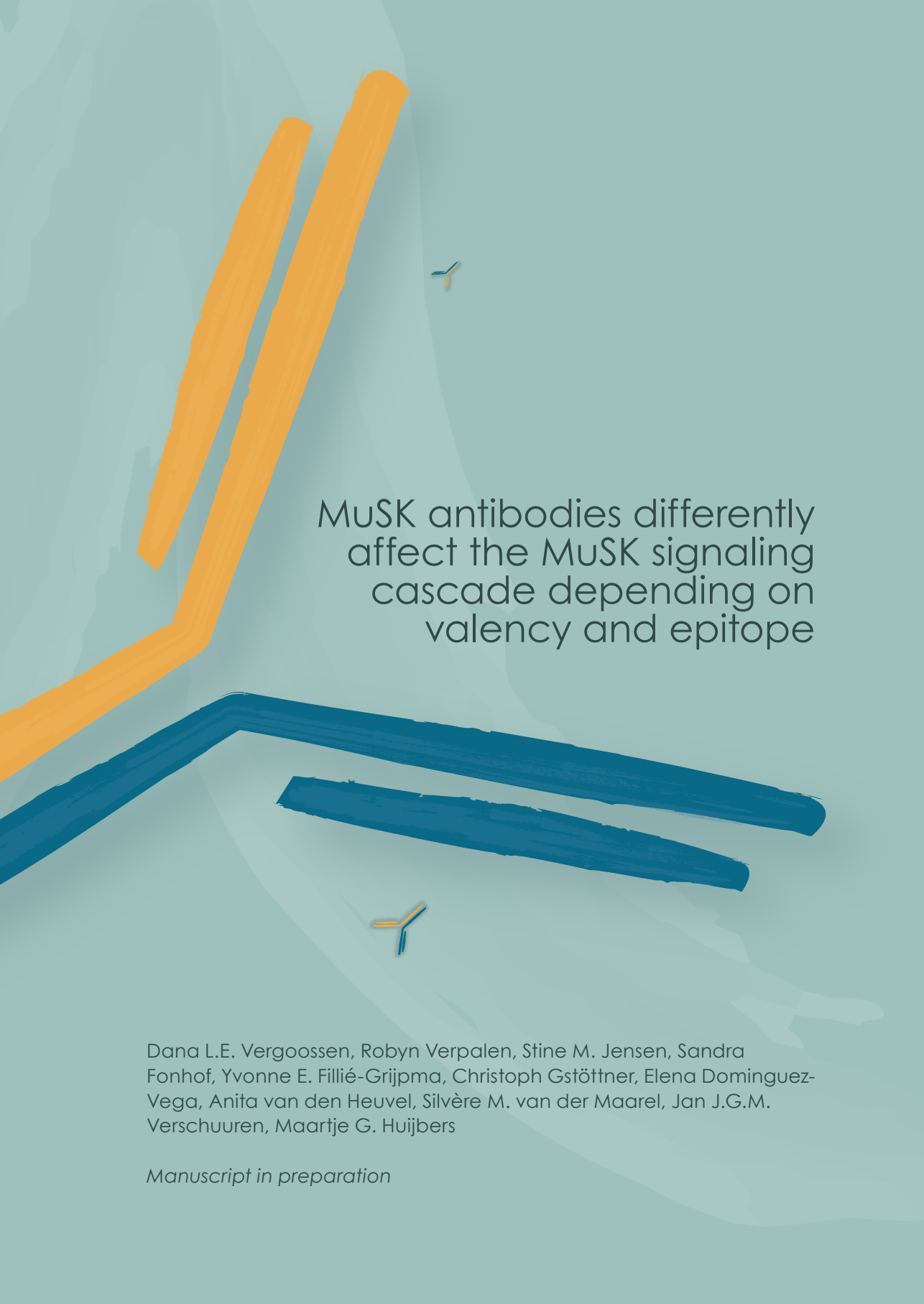
License: [Licence agreement concerning inclusion of doctoral thesis in the Institutional Repository of the University of Leiden](#)

Downloaded from: <https://hdl.handle.net/1887/3567889>

**Note:** To cite this publication please use the final published version (if applicable).

# 5



The background features abstract brushstrokes in orange and blue. Two orange strokes are in the upper left, and two blue strokes are in the lower right. Two small Y-shaped icons, one orange and one blue, are positioned near the center of the page.

# MuSK antibodies differently affect the MuSK signaling cascade depending on valency and epitope

Dana L.E. Vergoossen, Robyn Verpalen, Stine M. Jensen, Sandra Fonhof, Yvonne E. Fillié-Grijpma, Christoph Gstöttner, Elena Dominguez-Vega, Anita van den Heuvel, Silvère M. van der Maarel, Jan J.G.M. Verschuuren, Maartje G. Huijbers

*Manuscript in preparation*

**Abstract**

Muscle-specific kinase (MuSK) plays a central role in forming and maintaining healthy neuromuscular junctions (NMJ). Antibodies against MuSK impair MuSK functioning and thereby cause myasthenia gravis (MG). MuSK autoantibodies are predominantly IgG4, which bind in a monovalent fashion to MuSK due to Fab-arm exchange. Monovalent and bivalent MuSK antibodies have opposite effects on MuSK activation. How valency and other antibody characteristics affect MuSK's interaction with partner molecules and intracellular pathways downstream of MuSK is largely unknown. To further understand the pathogenic mechanisms underlying MuSK MG, we have investigated how MuSK antibody binding affects MuSK functioning with a panel of human (patient-derived) monoclonal MuSK antibodies. We found valency-dependent effects on inhibition of agrin-induced MuSK activation, Dok7 binding to MuSK and NMJ gene expression. Monovalent binding to the frizzled domain of MuSK did not inhibit agrin-induced MuSK activation, in contrast to binding to the Ig-like 1 domain. In addition, the kinetics of Dok7 degradation induced by bivalent MuSK antibodies appear to depend on epitope binding between and within structural domains of MuSK. None of the clones tested (both bivalent and monovalent) increased MuSK internalization. The net pathogenic effect of polyclonal MuSK antibodies in individual MuSK MG patients thus likely depends on autoantibody titer, and the unique composition of MuSK autoantibodies varying in epitope-binding and valency.

## Introduction

The neuromuscular junction (NMJ) is a specialized synapse where motor neurons and skeletal muscles communicate. Most proteins in the NMJ are indispensable as neuromuscular communication is essential for basic muscular functions such as breathing <sup>1</sup>. Muscle-specific kinase (MuSK) is a transmembrane tyrosine kinase which forms a central signaling hub essential for forming and actively maintaining the NMJ <sup>1</sup>. MuSK has three extracellular immunoglobulin-like (Ig-like) domains followed by a frizzled-like domain (Fz-domain), a transmembrane domain and an intracellular kinase domain <sup>2</sup>. The interaction between its Ig-like domain 1 and lipoprotein receptor-related protein 4 (Lrp4) is crucial for activation and autophosphorylation of the MuSK kinase domain through dimerization of two MuSK molecules <sup>3,4</sup>. The interaction between Lrp4 and MuSK is greatly enhanced once neuronal agrin released from the motor nerve terminal has bound Lrp4 <sup>4</sup>. Upon dimerization and autophosphorylation of MuSK, downstream of kinase 7 (Dok7) is recruited to the intracellular phosphotyrosine-binding site, stabilizing and enhancing phosphorylation of both MuSK and Dok7 <sup>5,6</sup>. This initiates further downstream signaling leading to cytoskeletal reorganization and clustering of acetylcholine receptors (AChRs) by scaffold protein rapsyn, and contributes to transcriptomic regulation of NMJ-specific genes <sup>1,7</sup>. In addition, the MuSK Ig-like 1 domain is involved in tethering the Collagen Q (ColQ) - acetylcholine esterase (AChE) complex to the NMJ <sup>8</sup>. AChE breaks down acetylcholine, the main neurotransmitter responsible for neurotransmission at the NMJ and thereby regulates neuromuscular communication. Because MuSK has multiple functions in the NMJ, perturbing or modifying its functioning can have many consequences.

Antibodies against MuSK cause the neuromuscular autoimmune disorder myasthenia gravis (MuSK MG) characterized by fatigable skeletal muscle weakness <sup>9</sup>. MuSK autoantibodies are predominantly of the IgG4 subclass and thus become in great majority bispecific and functionally monovalent through the stochastic process of Fab-arm exchange <sup>10-12</sup>. Besides IgG4 MuSK antibodies, some patients also have low levels of co-occurring functionally bivalent and monospecific IgG1, IgG2 or IgG3 MuSK antibodies <sup>10, 13, 14</sup>. The term “bivalent” will be used for functionally bivalent and monospecific antibodies and the term “monovalent” for functionally monovalent and bispecific antibodies. Bivalent MuSK antibodies can (partially) activate MuSK (agonists), while monovalent MuSK antibodies inhibit agrin-induced MuSK activation (antagonists) <sup>15-17</sup>. These opposing effects are related to the natural dimerization of MuSK

that occurs in a healthy synapse to keep the MuSK kinase constitutively active and the NMJ intact. Monovalent MuSK antibodies block Lrp4-MuSK interaction thereby preventing dimerization and activation of the kinase and AChR clustering leading ultimately to synaptic disintegration and skeletal muscle fatigue<sup>13, 18</sup>. In contrast, bivalent MuSK antibodies are thought to force dimerization of MuSK, therefore bypassing the need of agrin and Lrp4 in activating MuSK<sup>15, 19</sup>. Experiments with recombinant monoclonal antibodies based on anti-MuSK B-cell receptor (BCR) sequences isolated from MuSK MG patients show that monovalent MuSK antibodies are more pathogenic than their bivalent equivalents and cause rapid onset fatigable muscle weakness in mice<sup>16</sup>. However, the pathogenicity of bivalent MuSK antibodies varies between clones. While *in vitro* their AChR clustering capabilities are relatively equal, some bivalent MuSK antibodies can cause myasthenic muscle weakness with slower disease progression (compared to monovalent MuSK antibodies) in mice, while others are non-pathogenic, even after long-term exposure<sup>15, 16, 20</sup>. We therefore hypothesize that the mechanism by which MuSK antibodies impair MuSK signaling may differ between clones and depend on antibody valency.

Here we investigated the effect of six MuSK antibody clones in monovalent and bivalent format on Dok7, MuSK internalization and NMJ gene expression.

## Results

### *MuSK antibodies differentially affect MuSK and Dok7 depending on valency and epitope.*

To investigate how MuSK antibodies with different characteristics affect MuSK-mediated signaling, we generated a panel of six human recombinant MuSK antibodies (Figure 1A). The sequences of five MuSK clones were isolated from MuSK MG patient BCR sequences and one MuSK clone was identified after phage display selection and screening<sup>15, 21, 22</sup>. All clones were produced in a bivalent manner. Monovalent equivalents were generated by IgG4 controlled Fab-arm exchange with the b12 control antibody and are described as [clone]xb12<sup>16</sup>. The residual amount of bivalent MuSK antibody after the controlled Fab-arm exchange method was two percent or less, validating the relative purity of the monovalent MuSK antibodies (Figure S1A)<sup>16, 23</sup>. Due to Fab-glycosylation, the 11-3D9xb12 mixture was too complex to calculate relative amounts of each variant. However, the deconvoluted mass spectra in this mixture confirmed the generation of the bispecific,

monovalent variant for this clone (Figure S1B). Five out of six clones bind the Ig-like 1 domain of MuSK, while one clone (mAb13) binds the Fz domain<sup>15, 24</sup>.

C2C12 myotube cultures are a well-established cell model to interrogate MuSK signaling *in vitro* as they endogenously express the muscle-specific signaling components of this pathway. All five monovalent MuSK antibodies binding the Ig-like 1 domain of MuSK fully inhibited agrin-induced MuSK phosphorylation, while their bivalent equivalents do not (Figure 1B and C). Monovalent mAb13xb12 binding the Fz domain of MuSK did not inhibit MuSK phosphorylation, even at higher concentrations (Figure 1B, 1C and S2A). Bivalent mAb13 was able to induce MuSK phosphorylation in the absence of agrin, while monovalent mAb13xb12 was not (Figure S2B). For agrin in combination with bivalent 13-3B5 or mAb13, MuSK phosphorylation exceeded the levels of agrin with the b12 control antibody, while for bivalent 13-3D10 the MuSK phosphorylation levels were slightly lower (Figure 1B and C). This suggests that the bivalent MuSK antibody is facilitating MuSK phosphorylation over agrin. Taken together, the inhibition of MuSK by monovalent MuSK antibodies seems to depend on which the structural domain of MuSK is targeted, while the agonistic capacity of bivalent MuSK antibodies does not.

Dok7 binding to MuSK is critical to stabilize and enhance MuSK phosphorylation and propagate intracellular signaling<sup>5, 6</sup>. If Dok7 cannot properly bind to phosphorylated MuSK, this can contribute to antibody pathogenicity. To assess how much Dok7 interacts with MuSK upon MuSK antibody-binding, endogenously expressed MuSK was immunoprecipitated and assessed for co-immunoprecipitation of Dok7. Inhibition of MuSK phosphorylation by monovalent MuSK antibodies resulted in less Dok7 bound to MuSK compared to their bivalent equivalents for the MuSK Ig-like 1 binding 13-3B5, 11-3F6, 11-3D9 and 13-4D3 clones (Figure 1D). No large differences were found in the recruitment of Dok7 to MuSK between for the 13-3D10 and mAb13 clones and between individual bivalent or monovalent anti-MuSK clones. To investigate if equal amounts of Dok7 was available for binding to MuSK in all conditions, we investigated total Dok7 levels in whole cell lysate (WCL). Bivalent 13-3B5 and 11-3F6 significantly reduced Dok7 protein levels compared to agrin with their monovalent equivalents (Figure 1E). In addition, agrin with 13-3B5 has significantly lower Dok7 levels compared to agrin with control antibody b12. Tendencies for lower Dok7 levels compared to agrin were also seen for some of the other, especially bivalent, MuSK clones.

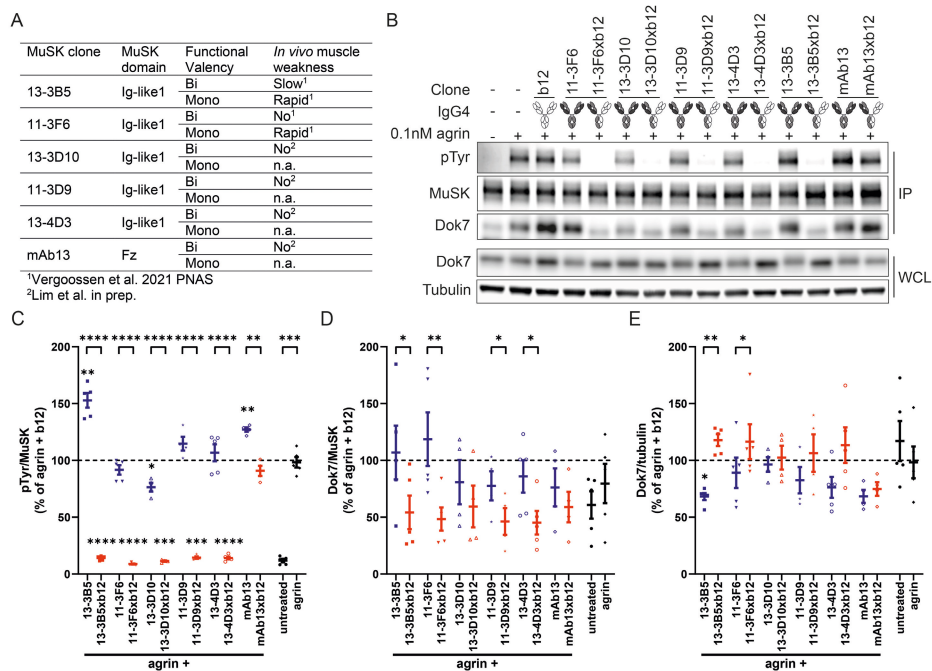


**Figure 1. MuSK antibodies differentially affect MuSK and Dok7 depending on valency and epitope.** **A.** Panel of anti-MuSK clones and variants with antibody characteristics. **B.** Representative blots of MuSK phosphorylation signal and MuSK-Dok7 co-immunoprecipitation. Quantification of phosphorylated MuSK (**C**), Dok7 interacting with MuSK (**D**) and Dok7 levels in whole cell lysate (**E**) after 30 min exposure. Data represents mean and SEM.  $n=5$  for 13-3B5(xb12), 11-3F6(xb12), 13-4D3(xb12) and agrin and  $n=4$  for 11-3D9(xb12), 13-3D10(xb12) and mAb13(xb12). Paired *t*-test on log-transformed data with Benjamini-Hochberg false discovery rate correction. IP = immunoprecipitation, WCL = whole cell lysate.

To further investigate the kinetics of how MuSK activation by bivalent MuSK antibodies or agrin influences Dok7, we measured Dok7 levels in whole cell lysate over time. Bivalent mAb13 reduced Dok7 most similarly to agrin, starting at 2 hours and continuing to 6 hours (Figure 2). In contrast, bivalent MuSK clones binding the Ig-like 1 domain already significantly reduced Dok7 levels after 30 minutes, but do not appear to further decrease Dok7 levels at later time points (Figure 2). Consistently, Dok7 levels upon 30-minute exposure to bivalent 13-3B5, 13-3D10 and 13-4D3 were significantly lower than mAb13 (Figure 2C). Bivalent 13-3B5 reduced Dok7 levels more than all other Ig-like 1 domain binding clones at 2 and 6 hours and compared to bivalent 11-3F6 at 30 minutes (Figure 2C-E). Bivalent mAb13 induced significantly lower Dok7 levels compared to the 13-3D10 and 13-4D3 clones at 6 hours (Figure 2E). Agrin induced significantly lower Dok7 levels compared to bivalent 13-3D10 at 6 hours,

but no other significant differences between agrin and the bivalent MuSK mAbs could be detected after correcting for multiple comparisons (Figure 2E). Since mAb13 binds the Fz domain and the 13-3B5 clone binds a non-overlapping epitope compared to the other Ig-like 1 domain binding clones, Dok7 levels appear to be affected differently by bivalent MuSK antibodies depending on antibody epitope<sup>20</sup>.

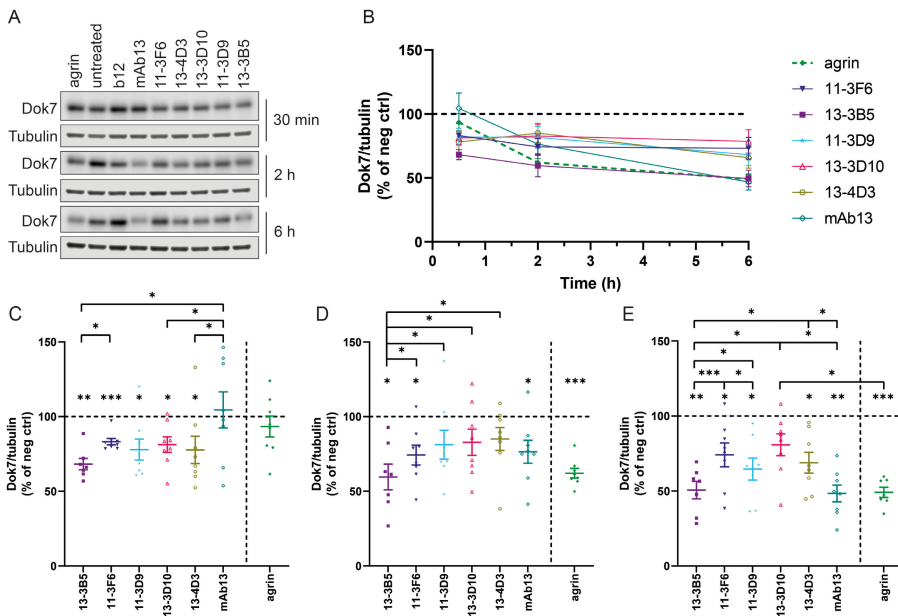


**Figure 2.** Bivalent MuSK antibodies affect Dok7 levels differently over time depending on epitope and clone. A. Representative blots of Dok7 levels at 30 min, 2 h and 6 h. Quantification of Dok7 levels over time (B), after 30 min (C), 2 h (D) and 6 h (E). Data represents mean and SEM and is normalized against b12 for MuSK mAbs, and against untreated for agrin. n=8 (except for 13-3B5 n=7) for 30 min and 2 h, n=8 (except for untreated, agrin and 13-3B5 n=7) for 6h. Paired t-tests on log-transformed data with Benjamini-Hochberg false discovery rate correction.

**MuSK antibodies do not deplete MuSK from the membrane of C2C12 myotubes**

To get more detailed understanding on what determines the pathogenicity of MuSK antibodies, we studied the 13-3B5 and 11-3F6 clones further. They differ in pathogenic capacity in bivalent form while binding the same domain of MuSK, preventing confounding effects of different target domains on MuSK<sup>16</sup>. Accelerated internalization is a common consequence of antigen-crosslinking by bivalent antibody binding. In addition, multiple receptor tyrosine kinases are known to rapidly internalize upon activation<sup>25</sup>. If MuSK is depleted from the membrane by antibody binding, this can contribute the pathogenicity

of MuSK antibodies. To investigate whether the amount of endogenously expressed MuSK on the membrane surface is affected by exposure to MuSK antibodies, we biotinylated and pulled down membrane surface proteins of C2C12 myotubes and probed this fraction for MuSK immunoreactivity. Neither monovalent nor bivalent MuSK antibodies binding the Ig-like 1 domain reduced the amount of surface MuSK after 30 minutes of exposure (Figure 3). Agrin, at the minimal dose for maximal activation (0.11nM) or a supramaximal dose (5nM), also did not reduce the amount of surface MuSK. Exposure to epidermal growth factor (EGF) for 15 minutes did significantly reduce the amount of surface EGF receptor in C2C12s, validating the method. Longer exposure to agrin or bivalent 13-3B5 also did not reduce endogenous MuSK on the surface membrane (Figure S3). Thus, the amount of MuSK on the membrane seems stable during active signaling and is not altered by exposure to these antibodies in C2C12 myotubes.

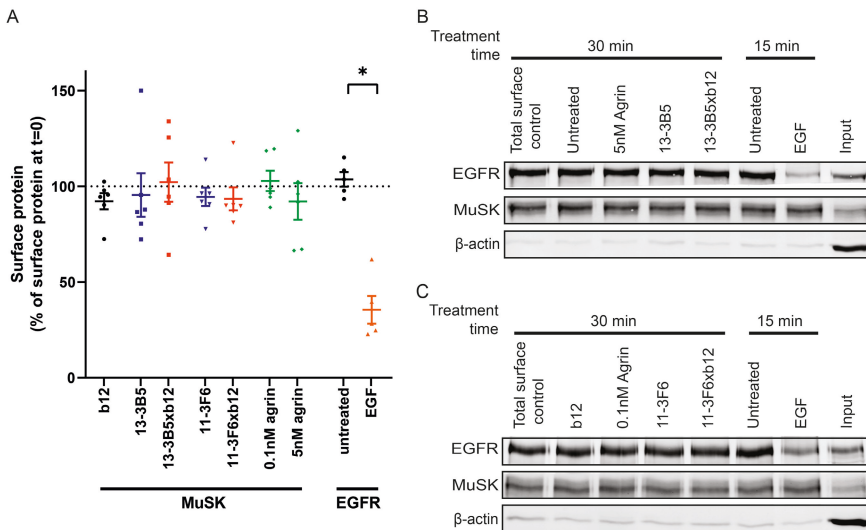


**Figure 3: MuSK surface depletion does not occur following exposure to monovalent or bivalent MuSK antibodies.** A. Quantification of surface MuSK following 30 min exposure to monovalent or bivalent MuSK antibodies or agrin compared to t=0 in C2C12 myotubes (n=6). Significant surface depletion of the EGFR following EGF exposure could be detected with this method (n=5). Representative blots of surface MuSK and EGFR upon 13-3B5(xb12) (B) or 11-3F6(xb12) (C). Intracellular protein  $\beta$ -actin is not pulled down with this method. Data depicts mean  $\pm$  SEM. Paired t-test on log-transformed data with Holm-Bonferroni correction.

***Neuromuscular junction gene expression is differentially affected by monovalent and bivalent MuSK antibodies.***

Expression of synaptic genes for the specialized structure and function of the NMJ is tightly regulated and specific to subsynaptic nuclei in the synaptic region of muscles<sup>7</sup>. Disruptions in their expression may contribute to the pathomechanism of disease-causing MuSK antibodies. To investigate if altered NMJ gene expression may explain the pathogenic differences observed between MuSK antibodies, we measured RNA expression of NMJ genes with a direct link to MuSK signaling in masseter muscle of NOD/SCID mice exposed for 11 days or 3 weeks to bivalent or monovalent MuSK antibodies<sup>16</sup>. Briefly, monovalent MuSK antibodies to the Ig-like 1 domain caused severe myasthenic muscle weakness, lethal after 11 days (Figure 4A). In contrast, bivalent 11-3F6 did not cause overt muscle weakness after 3 weeks, while exposure to bivalent 13-3B5 resulted in subclinical myasthenic muscle weakness after 11 days progressing to lethal muscle weakness after 3 weeks of exposure<sup>16</sup>.

Monovalent and bivalent MuSK antibodies caused different patterns of NMJ gene expression in the masseter muscle. In general, monovalent MuSK antibodies showed a (tendency to) decreased expression of a subset NMJ genes, while bivalent MuSK antibodies (a tendency to) increased expression of not exactly the same NMJ genes (Figure 4B). MuSK antibodies differentially affected the expression of *Lrp4*, *Chrne*, *Chrng*, *Colq* and *Ache* depending on valency. Most notably, monovalent MuSK antibodies strongly downregulated *Colq*, *Ache* and the epsilon subunit of the AChR (*Chrne*), while bivalent MuSK antibodies even after prolonged exposure did not (Figure 4G, J and K). In contrast, both bivalent MuSK antibodies strongly increased the expression of the gamma subunit of the AChR (*Chrng*), while this was not caused by exposure to monovalent MuSK antibodies at end-stage disease (Figure 4H). The alpha 1 subunit of the AChR (*Chrna1*) was only increased by bivalent 13-3B5 after 3 weeks of exposure (Figure 4F). Lastly, *Musk* is the only gene with a trend ( $p=0.07$ ) to increased expression for all MuSK antibodies (both monovalent and bivalent) that caused a myasthenic phenotype (Figure 4D). Taken together, these data further support monovalent and bivalent MuSK antibodies cause myasthenic muscle weakness through different mechanisms.

MuSK-mediated signaling is involved in regulating NMJ-specific gene expression in subsynaptic nuclei<sup>7</sup>. To investigate if MuSK antibody binding directly affects (NMJ) gene expression in muscle, we measured the total RNA transcriptome of C2C12 myotubes exposed to agrin, bivalent 13-3B5, or agrin in combination with monovalent 13-3B5xb12 or 11-3F6xb12 for 16h, as at this time the full AChR clustering cascade is on.

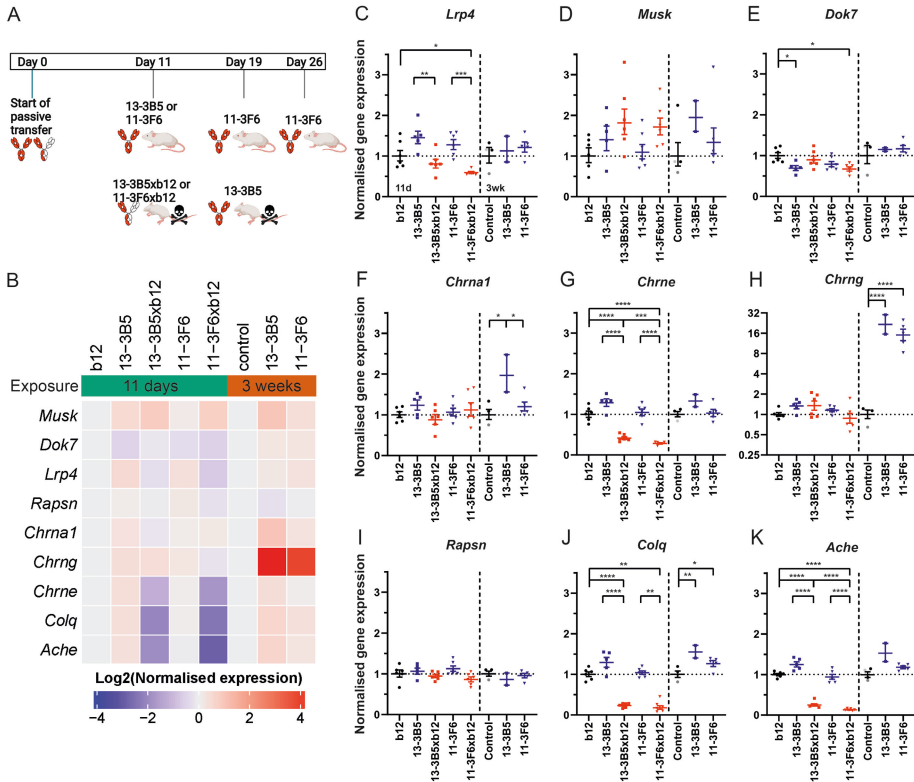


Figure 4: Monovalent and bivalent MuSK antibodies have differential effects on NMJ gene expression in mouse muscle. A. Graphic summary of results and time frame of passive transfer experiments <sup>16</sup> B. Log<sub>2</sub> normalised expression of NMJ genes in masseter muscle of NOD/SCID mice exposed to MuSK antibodies. Normalised gene expression of *Lrp4* (C), *Musk* (D), *Dok7* (E), *Chrna1* (F), *Chrne* (G), *Chrng* (H), *Rapsn* (I), *Colq* (J), *Ache* (K) in masseter muscle of exposure to MuSK antibodies for 11 days (left of dotted line) or 3 weeks (right of dotted line). Data depicts geometric mean  $\pm$  geometric SEM. 11 days: 2.5mg/kg b12, 13-3B5xb12, 11-3F6, 11-3F6xb12: n=6; 2.5mg/kg 13-3B5: n=5. 3 weeks: control is 10mg/kg b12 (black): n=2 combined with untreated or PBS-treated (grey): n=2; 10mg/kg 13-3B5: n=2; 10mg/kg 11-3F6: n=5. One-way ANOVA with Šidák-corrected comparisons for 11 day exposure. One-way ANOVA with Fisher's LSD test for 3 week exposure. Welch ANOVA when assumption of equal variance was not met. \* $p < 0.05$ , \*\* $p < 0.01$ , \*\*\* $p < 0.001$ , \*\*\*\* $p < 0.0001$

No differentially expressed genes were found upon MuSK activation or MuSK-antibody binding (data not shown). To confirm we did not miss the gene expression window induced by MuSK signaling, we exposed C2C12s to agrin or bivalent MuSK antibodies for different durations between 30 minutes and 24 hours and measured the expression of *Chrne* and *Musk*, because their promoters have experimentally been shown to be directly regulated by MuSK signaling <sup>26, 27</sup>. MuSK activation by agrin or bivalent MuSK antibodies did not affect *Chrne* or *Musk* expression within

24 hours (Figure S4A and B). Neuregulin activates the other pathway regulating NMJ gene expression in muscles and did rapidly increase the expression of early growth response 3 (*Egr3*) and showed a tendency to increase *Chrne* expression after 24 hours (Figure S4A and C) <sup>7</sup>. This suggests gene expression changes relevant for the NMJ can be detected in C2C12 myotubes however, those mediated through MuSK may require more time. Exposure to MuSK activating compounds for more than 24 hours resulted in cell death, hindering the investigation of longer-term or indirect effects of MuSK signaling on gene expression. Taken together, the observed changes in NMJ gene expression in the masseter muscle are unlikely to be mediated by an acute effect of MuSK-antibody binding on MuSK signaling.

## Discussion

To further understand the mechanisms underlying MuSK MG, we tested how a panel of monovalent and bivalent (patient-derived) monoclonal MuSK antibodies affected MuSK-mediated signaling. Our data support the conclusion that the valency and epitope of MuSK antibodies have a significant effect on MuSK activation, Dok7 and NMJ gene expression.

MuSK antibodies binding the Ig-like 1 domain have valency-dependent effects on MuSK activation and Dok7. Monovalent MuSK antibodies inhibited agrin-induced MuSK phosphorylation and Dok7 binding to MuSK, while their bivalent equivalents induced these processes, confirming and extending on previous findings on MuSK phosphorylation <sup>15-17</sup>. These data support that the forced dimerization of MuSK by bivalent MuSK antibodies allows for Dok7 binding to the intracellular domain of MuSK. The expression of several NMJ genes was also differentially affected depending on MuSK antibody valency. Monovalent, but not bivalent, MuSK antibodies decreased the gene expression of *Colq*, *Ache* and *Chrne* and to a lesser extent *Lrp4*. In contrast, bivalent, but not monovalent, MuSK antibodies greatly increased *Chrng* expression, similar to what was seen upon active immunization with MuSK <sup>28</sup>. Murine antibody subclasses are not able to undergo Fab-arm exchange, therefore all antibodies in active immunization animal models are bivalent. Congruent with this, *Colq*, *Ache* and *Chrne* expression was not reduced upon MuSK active immunization <sup>28</sup>. Thus, the cellular consequences of monovalent and bivalent MuSK antibodies differ considerably also beyond the MuSK-induced AChR clustering pathway. Importantly, this emphasizes that active immunization and passive transfer studies of MuSK MG are models for considerably different aspects of the disease mechanisms in humans.

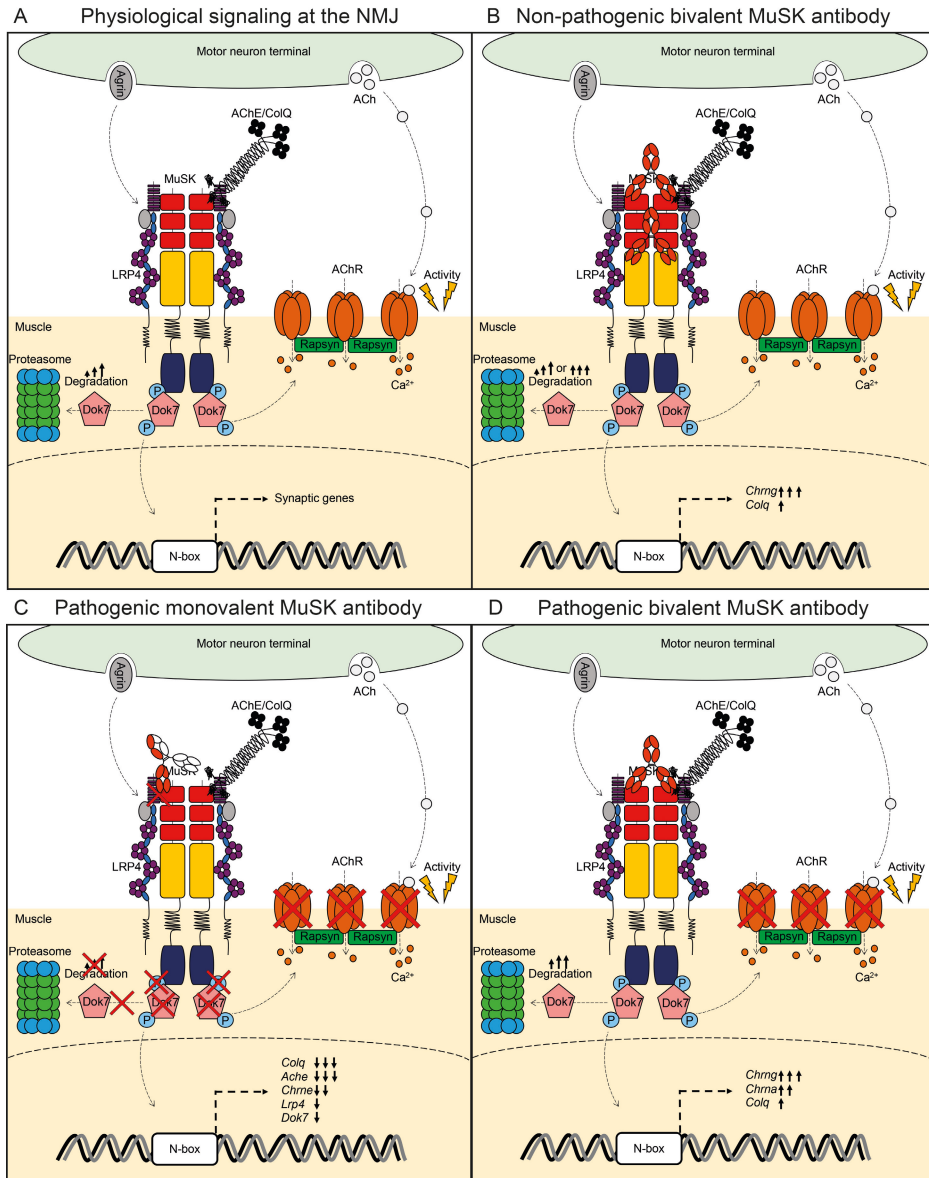


Figure 5: Model of how MuSK antibodies with different functional characteristics impact signaling at the NMJ. A. During physiological signaling agrin-Lrp4 dimerizes and autophosphorylates MuSK. Dok7 binds to phosphorylated MuSK and is phosphorylated itself initiating a signaling cascade leading to clustering of AChR. In addition, MuSK binds ColQ-AChE complex, tethering it to the synapse, and MuSK is involved in the expression of synaptic genes. Activity-dependent degradation of Dok7 over time may be the break of this signaling cascade. B. Non-pathogenic bivalent MuSK antibodies have some effects on MuSK signaling, but these are not sufficient to cause dysfunction of neurotransmission. Pathogenic monovalent (C) and bivalent (D) MuSK antibodies have completely different effects on MuSK functioning, though both ultimately cause declustering of AChRs and myasthenic symptoms.

The antagonistic effects of monovalent MuSK antibodies on agrin-induced MuSK signaling seem epitope-dependent. All monovalent anti-MuSK clones binding the Ig-like 1 domain inhibited agrin-induced MuSK phosphorylation, while monovalent mAb13xb12 binding to the Fz domain did not. Previously, monovalent Fabs of MuSK antibodies binding the Ig-like 2 domain fully inhibited agrin-induced AChR clustering, while their bivalent equivalents partially inhibited AChR clustering and did not inhibit agrin-induced MuSK phosphorylation, similar to Ig-like 1 domain binders<sup>15, 16, 29, 30</sup>. Polyclonal patient IgG4 mainly targets the N-terminal Ig-like 1 and Ig-like 2 domains of MuSK, is estimated to be up to 99% monovalent and also blocks agrin-induced MuSK activation and AChR clustering<sup>11, 13, 18, 31</sup>. Congruent with these *in vitro* effects, polyclonal patient IgG(4) and monovalent MuSK monoclonal antibodies targeting the MuSK Ig-like 1 domain cause myasthenia in experimental animals<sup>16, 32, 33</sup>. Monovalent Fz-domain binders are expected to not be pathogenic *in vivo* because they do not inhibit agrin-induced MuSK activation, indicating epitope-dependent antibody pathogenicity of monovalent MuSK antibodies.

Bivalent MuSK antibodies binding the Ig-like 1 and Fz domain appear to differentially regulate cellular Dok7 levels, despite similar effects on MuSK activation and Dok7 binding to MuSK. Upon agrin-induced signaling, Dok7 is ubiquitinated and degraded in the proteasome, reducing cellular Dok7 levels<sup>17, 34</sup>. This is thought to be a crucial negative feedback loop in regulating agrin-induced MuSK signaling. Bivalent MuSK antibodies to the Ig-like 1 domain appear to reduce Dok7 levels faster compared to bivalent mAb13 binding the Fz domain and agrin, suggesting Dok7 is more rapidly degraded. Less Dok7 thus seems to be available soon after initiation of MuSK activation, potentially quickly dampening further downstream signaling. In addition, bivalent 13-3B5 resulted in the largest reduction of Dok7 compared to the other Ig-like 1 domain binding clones at all time points. Since bivalent 13-3B5 binds a non-overlapping epitope on the Ig-like 1 domain compared to Ig-like 1 domain binders, this suggests that differences in epitope within a structural domain of MuSK can also have functional consequences<sup>20</sup>. In sum, these results support MuSK can be dimerized and activated differently depending on antibody-epitope between and within structural MuSK domains, influencing the kinetics of Dok7 degradation and potentially further downstream signaling.

These valency- and epitope-dependent effects on MuSK signaling confirm earlier studies that inhibition of agrin-induced MuSK activation, by blocking the interaction between Lrp4 and MuSK, is the driving

pathomechanism of monovalent MuSK antibodies (Figure 5)<sup>13, 18, 35</sup>. The strong reduction in *Chrne*, *Colq* and *Ache* expression levels by monovalent MuSK antibodies in addition suggests a production shortage of both mature AChRs and the ColQ-AChE complex. The latter may contribute to the deleterious effects of AChE inhibitors in MuSK MG patients and passive transfer models<sup>36, 37</sup>. Monovalent MuSK antibodies binding the Ig-like domain 1 may thus interfere with ColQ-AChE functioning by reducing the amount of the ColQ-AChE complex in the NMJ on one hand, and through inhibiting its tethering to the postsynaptic structure by blocking MuSK-ColQ interaction on the other hand<sup>38</sup>. The inhibition of MuSK thus has consequences throughout the NMJ that determine clinical symptoms and treatment response.

The driving mechanisms of pathogenic bivalent MuSK antibodies are still less clear. The strong upregulation of *Chrng* expression after 3 weeks may be a sign of presynaptic denervation of the NMJs<sup>39, 40</sup>. However, abnormalities in presynaptic morphology were not observed at 11 days (congruent with the lack of *Chrng* expression at that time), while postsynaptic pathology was already present in both bulbar and a limb muscle<sup>16</sup>. In addition, *Chrng* expression was also upregulated by non-pathogenic 11-3F6, suggesting any potential presynaptic pathology is unlikely to drive the pathogenicity of bivalent MuSK antibodies. The early and relatively large reduction of *Dok7* levels in C2C12s by pathogenic 13-3B5 may indicate *Dok7* is degraded too much too quickly upon activation, hampering further downstream signaling and supporting previous findings with polyclonal bivalent anti-MuSK IgG from rabbits (Figure 5)<sup>17</sup>. Fast depletion of *Dok7* may contribute to the pathogenicity of bivalent MuSK antibodies, since *Dok7* is essential for the activation of MuSK and proper downstream signaling<sup>5, 17</sup>. However, the differences between pathogenic 13-3B5 and the non-pathogenic bivalent MuSK antibodies or agrin were not all statistically significant (after correction for multiple comparisons) at the earliest time-point, and 13-3B5 and agrin are very similar at the later timepoints. The effects are thus time-dependent and the consequences for further downstream signaling should be investigated further to understand if *Dok7* depletion contributes to mechanisms underlying pathogenic bivalent MuSK antibodies.

Endogenous MuSK did not deplete from the surface membrane after either monovalent or bivalent MuSK antibody binding or activation in C2C12s. Recently, agrin caused a slow decrease leading to ~30% loss of surface MuSK when protein synthesis was inhibited<sup>41</sup>. Protein synthesis was not inhibited in our assay. Thus, continuous synthesis and integration of

MuSK into the membrane may compensate this loss of MuSK, stabilizing the amount of MuSK on the membrane surface. This may explain why we could not reproduce loss of surface MuSK observation, despite using similar experimental settings. Gemza et al. furthermore elegantly discuss this slow rate of MuSK endocytosis in relation to previous studies and other receptor tyrosine kinases may be due to 1) the indirect activation of MuSK through Lrp4 and Dok7 and 2) anchoring of MuSK in the dense cytoskeletal structure of the post-synapse<sup>25, 41, 42</sup>. Furthermore, internalization of exogenous MuSK by MuSK patient-purified IgG(4) has not been consistently found<sup>18, 43</sup>. This may depend on the activating vs inhibiting properties of the material used and/or overestimation of internalization due to overexpression of MuSK and/or the absence of the relevant muscle-specific cytoskeletal structure. Taken together, rapid antibody-mediated or activity-dependent surface depletion of MuSK is unlikely to be a major part of the mechanism of either monovalent or bivalent MuSK antibody pathogenicity in muscle.

Of note, MuSK signaling or MuSK antibodies also did not directly alter (NMJ) gene expression in C2C12 myotubes. Previously, agrin-induced signaling was found to activate the *Musk* promoter directly through MKK7, JNK and GABP signaling<sup>26</sup>. In that study, agrin was coated onto the culture dish in combination with laminin from the beginning of myotube differentiation, as opposed to supplied in the media to differentiated myotubes. This suggests that this signaling pathway is not directly activated upon agrin-induced MuSK activation but requires longer. This idea is supported by the absence of MKK7, JNK and GABP phosphorylation 2 hours after stimulation, when MuSK, Dok7 and AChR phosphorylation are already present<sup>44</sup>. Although, MuSK antibodies affect NMJ gene expression in the masseter muscle at end-stage disease, the signaling responsible for this may require longer and be more complex downstream of MuSK activation.

Taken together, MuSK MG patients have a polyclonal antibody response resulting in a mixture of MuSK antibodies against different epitopes, and of subclasses differing in valency and complement activating capacity. The net effect of MuSK autoantibodies in individual MuSK MG patients will be determined by the unique composition of MuSK antibodies and their characteristics, in combination with their relative titres. It will be interesting to get a more in dept view on the heterogeneity and clonality of the MuSK autoantibody response in individual patients and to study if these characteristics can explain the severity of the clinical symptoms.

## Methods

### *mAb production and cFAE*

Anti-MuSK clones binding to the Ig-like domain 1 of MuSK were previously isolated from a MuSK MG patient<sup>15</sup>. Together with mAb13 as a MuSK Fz domain binder, these clones were produced in an IgG4 Fc tail with the S228P amino-acid change and their original light chain (GeneArt,<sup>16,21,22</sup>). The b12 antibody suitable for cFAE was used as an exchange partner and control antibody<sup>16</sup>. Recombinant bivalent and monovalent monoclonal antibodies (mAbs) were produced, quantified and assessed on quality as described previously<sup>15,16</sup>. Recombinant antibodies 11-3F6, 13-3B5 and b12 were produced in CHO cells. The other MuSK mAbs were produced in HEK cells.

### *C2C12 culturing and treatment conditions*

C2C12 myoblasts were obtained from CLS Cell Lines Service GmbH (Eppelheim, Germany), tested for mycoplasma contamination and maintained for maximum 5 passages after thawing. Myoblasts were grown in proliferation medium (DMEM Glutamax (10566016, Thermo Fisher) supplemented with 10% FBS (S1810-500, Biowest) and 1% penicillin/streptomycin (15140122, Gibco). Cells were plated at  $1.25 \times 10^4$  –  $2 \times 10^4$  cells per  $\text{cm}^2$  in proliferation medium. Once cells reached 90 – 95 % confluency, differentiation was induced by DMEM Glutamax supplemented with 2% HS and 1% penicillin/streptomycin, refreshed every 2-3 days. Experiments were done on day 5 of differentiation. All mAbs were used at 7.7nM, neural agrin (550-AG-100, R&D systems) at 0.1nM, neuregulin (396-HB-050, R&D systems) at 4.9nM, EGF at 200ng/mL (236-EG-200, R&D systems), unless otherwise specified.

### *MuSK immunoprecipitation*

MuSK was immunoprecipitated (IP) as described previously<sup>16</sup>. Briefly, differentiated C2C12 myotubes were cultured in 10cm dishes, treated for 30 min and lysed in phosphate lysis buffer (30 mM triethanolamine, 1% NP 40, 50mM NaF, 2mM sodium orthovanadate, 1mM sodium tetrathionate, 5 mM EDTA, 5 mM EGTA, 1mM N-ethylmaleimide, 50mM NaCl, 1× protease inhibitor cocktail, 1× phosphatase inhibitor cocktail). Lysates were cleared by centrifuging for 20 min at 5.000 g, adjusted to ensure equal protein input over all conditions and combined with 1µg/sample 11-3F6 IgG1 to IP MuSK. Antibody-protein complexes were captured with protein a agarose beads (11134515001, Roche) and eluted with 40-50µL 2x sample buffer (40mM Tris-HCl pH6.8, 3.3% SDS, 16.5% glycerol, 0.005% Bromophenol blue, 0.2M DTT) and incubated at 95 degrees for 5 min.

### *Protein isolation*

To assess Dok7 levels, C2C12 myotubes were cultured in 6-well plates. After treatment, myotubes were harvested in ice-cold PBS and stored as cell pellets at -80 prior to protein isolation. Pellets were lysed in RIPA buffer (50mM Tris pH 7.4, 150mM NaCl, 1mM EDTA, 0.1% SDS, 1% NP-40, 0.5% sodium deoxycholate, 1x protease inhibitor cocktail) and cleared by centrifuging for 20 min at 5.000 g. Protein content of lysate was determined using BCA protein assay kit (23225, Thermo Scientific) and used to prepare samples with equal protein content in sample buffer.

### *Surface depletion assay*

Immediately after treatment exposure, cells were put and kept on ice in the cold room (4°C) until lysis. Cells were thoroughly washed with ice cold PBS<sup>2+</sup> (1.5mM MgCl<sub>2</sub>; 0.2mM CaCl<sub>2</sub> in PBS, pH 7.4). Freshly prepared 1mg/mL Sulfo-NHS-SS-Biotin (PG82077, Thermo Fisher) in PBS<sup>2+</sup> was added to each plate and incubated shaking vigorously (~300 rpm) for 30 min. Unbound Sulfo-NHS-SS-Biotin was washed away with quenching buffer (100mM Glycine in PBS<sup>2+</sup>) by rinsing three times and incubating shaking for 2x 15 minutes. All cells were washed three times with ice cold PBS<sup>2+</sup> before being lysed with RIPA buffer (10 mM Tris, pH 7.4; 150 mM NaCl; 1 mM EDTA; 0.1% SDS; 1.0% triton X-100; 1.0% sodium deoxycholate, 1x protease inhibitor cocktail). Lysates of all samples were adjusted to ensure equal protein input over all conditions based on BCA quantification. Adjusted lysates were incubated with streptavidin beads (20349, Thermo Scientific) rotating ON (4°C). Protein was eluted from the beads using 2x sample buffer.

### *Western blotting*

Protein samples were ran on SDS-PAGE gel and transferred to PDVF membrane. Western blot conditions for different samples types can be found in Table S1. Chemiluminescence was measured on the Amersham Imager 600 (Cytiva). Immunofluorescence was measured with the Odyssey (Licor).

### *RNA isolation*

C2C12 myotubes or frozen muscle tissue were lysed and homogenized in QIAzol lysis reagent (Qiagen). Total RNA was extracted and purified with the miRNeasy Mini Kit according to manufacturer's instructions (Qiagen, 1038703). RNA was treated with DNase (Qiagen) on column for 30 min at room temperature. RNA concentration was quantified using NanoDrop ND-1000 spectrophotometer (Thermo Fisher Scientific).

### *Quantitative Real-time PCR*

First strand cDNA was synthesized from 1000-3000 ng total RNA with the RevertAid H Minus First Strand cDNA Synthesis kit using oligo(dT) primers (Thermo Fisher Scientific, K1632). Relative gene expression levels were determined with iQ SYBR Green Supermix (Bio-Rad, #1708886) and 1 pM forward and reverse primers (Table S2) on CFX384 Touch Real-Time PCR Detection System (Bio-Rad) with the following program: 95°C for 3 min, 40 cycles of 10 s at 95°C and a melting temperature of 60°C for 30 s, followed by a melting curve analysis from 65°C to 95°C (temperature increments of 0.5°C). Quantification cycle (Cq) values were obtained from CFX manager or maestro software (BioRad). All samples were run in triplicate and *Gapdh* and *Rpl13a* were used as housekeeping genes. Technical replicates that differed >0,5 in Cq from the others in the triplicate were excluded. Normalized fold changes were calculated compared to untreated or b12 using the validated efficiency of each primer (Table S2).

### *Bulk RNA sequencing and analysis*

Total RNA integrity of the 16 h-treated C2C12 myotube samples was analyzed with the Agilent BioAnalyzer RNA Nano 6000 chip and all had an RNA Integrity Number of > 9.5 (Agilent Technologies, Amstelveen, the Netherlands). The library was prepared with the TruSeq Stranded Total RNA with Ribo-Zero H/M/R kit and 30 million reads were sequenced with the NovaSeq 6000 PE 150 system (Illumina) by Macrogen. Reads were trimmed and quality filtered by TrimGalore (v.0.6.6, Cutadapt v.2.10), using default parameters to remove low-quality nucleotides. Consequently, reads were mapped to the Genome Reference Consortium Mouse Build 38, using STAR Aligner (v.2.7.6a). A gene expression counts table was generated with HTSeq (v.0.12.4). Data were normalized for sequencing depth with the median of ratios method and consequently analyzed for differential expression in the DESeq2 R package (v.1.32.0). Genes with an adjusted p-value < 0.05 (Benjamini-Hochberg) were considered significant.

### *Statistics*

Statistical analyses were done in GraphPad Prism software (version 9.3.1). Which statistical test was used per experiment is described in the figure legends. Data is presented as (geometric) mean with (geometric) standard error of the mean. p values <0.05 were considered significant. \*p < 0.05; \*\*p < 0.01; \*\*\*p < 0.001; \*\*\*\*p < 0.0001.

## References

1. Burden SJ, Huijbers MG, Remedio L. Fundamental Molecules and Mechanisms for Forming and Maintaining Neuromuscular Synapses. *Int J Mol Sci* 2018;19.
2. Valenzuela DM, Stitt TN, Distefano PS, et al. Receptor tyrosine kinase specific for the skeletal muscle lineage: expression in embryonic muscle, at the neuromuscular junction, and after injury. *Neuron* 1995;15:573-584.
3. Stiegler AL, Burden SJ, Hubbard SR. Crystal structure of the agrin-responsive immunoglobulin-like domains 1 and 2 of the receptor tyrosine kinase MuSK. *Journal of Molecular Biology* 2006;364:424-433.
4. Zhang W, Coldefy AS, Hubbard SR, Burden SJ. Agrin binds to the N-terminal region of Lrp4 protein and stimulates association between Lrp4 and the first immunoglobulin-like domain in muscle-specific kinase (MuSK). *J Biol Chem* 2011;286:40624-40630.
5. Okada K, Inoue A, Okada M, et al. The muscle protein Dok-7 is essential for neuromuscular synaptogenesis. *Science* 2006;312:1802-1805.
6. Inoue A, Setoguchi K, Matsubara Y, et al. Dok-7 activates the muscle receptor kinase MuSK and shapes synapse formation. *Science Signaling* 2009;2:ra7.
7. Belotti E, Schaeffer L. Regulation of Gene expression at the neuromuscular Junction. *Neurosci Lett* 2020;735:135163.
8. Cartaud A, Strohlic L, Guerra M, et al. MuSK is required for anchoring acetylcholinesterase at the neuromuscular junction. *The Journal of Cell Biology* 2004;165:505-515.
9. Evoli A, Tonali PA, Padua L, et al. Clinical correlates with anti-MuSK antibodies in generalized seronegative myasthenia gravis. *Brain* 2003;126:2304-2311.
10. McConville J, Farrugia ME, Beeson D, et al. Detection and characterization of MuSK antibodies in seronegative myasthenia gravis. *Ann Neurol* 2004;55:580-584.
11. Koneczny I, Stevens JA, De Rosa A, et al. IgG4 autoantibodies against muscle-specific kinase undergo Fab-arm exchange in myasthenia gravis patients. *J Autoimmun* 2017;77:104-115.
12. Van Der Neut Kolfschoten M, Schuurman J, Losen M, et al. Anti-inflammatory activity of human IgG4 antibodies by dynamic Fab arm exchange. *Science* 2007;317:1554-1557.
13. Koneczny I, Cossins J, Waters P, Beeson D, Vincent A. MuSK myasthenia gravis IgG4 disrupts the interaction of LRP4 with MuSK but both IgG4 and IgG1-3 can disperse preformed agrin-independent AChR clusters. *PLoS One* 2013;8:e80695.
14. Ohta K, Shigemoto K, Fujinami A, Maruyama N, Konishi T, Ohta M. Clinical and experimental features of MuSK antibody positive MG in Japan. *Eur J Neurol* 2007;14:1029-1034.
15. Huijbers MG, Vergoossen DL, Fillie-Grijpma YE, et al. MuSK myasthenia gravis monoclonal antibodies: Valency dictates pathogenicity. *Neurol Neuroimmunol Neuroinflamm* 2019;6:e547.
16. Vergoossen DLE, Plomp JJ, Gstöttner C, et al. Functional monovalency amplifies the pathogenicity of anti-MuSK IgG4 in myasthenia gravis. *Proc Natl Acad Sci U S A* 2021;118:2020.2009.2024.296293.
17. Mori S, Yamada S, Kubo S, et al. Divalent and monovalent autoantibodies cause dysfunction of MuSK by distinct mechanisms in a rabbit model of myasthenia gravis. *J Neuroimmunol* 2012;244:1-7.
18. Huijbers MG, Zhang W, Klooster R, et al. MuSK IgG4 autoantibodies cause myasthenia gravis by inhibiting binding between MuSK and Lrp4. *Proc Natl Acad Sci U S A* 2013;110:20783-20788.
19. Vergoossen DLE, Augustinus R, Huijbers MG. MuSK antibodies, lessons learned from poly- and monoclonality. *J Autoimmun* 2020;112:102488.

20. Lim JL, Augustinus R, Plomp JJ, et al. Development and characterization of agonistic monoclonal antibodies targeting the Ig-like 1 domain of muscle-specific kinase. in preparation.
21. Xie M-H, Yuan J, Adams C, Gurney A. Direct demonstration of MuSK involvement in acetylcholine receptor clustering through identification of agonist ScFv. *Nature Biotechnology* 1997;15:768-771.
22. Sengupta-Ghosh A, Dominguez SL, Xie L, et al. Muscle specific kinase (MuSK) activation preserves neuromuscular junctions in the diaphragm but is not sufficient to provide a functional benefit in the SOD1(G93A) mouse model of ALS. *Neurobiol Dis* 2019;124:340-352.
23. Gstöttner C, Vergoossen DLE, Wuhrer M, Huijbers MG, Domínguez-Vega E. Sheathless CE-MS as tool for monitoring exchange efficiency and stability of bispecific antibodies. *Electrophoresis* 2020.
24. Cantor S, Zhang W, Delestree N, Remedio L, Mentis GZ, Burden SJ. Preserving neuromuscular synapses in ALS by stimulating MuSK with a therapeutic agonist antibody. *eLife* 2018;7:e34375.
25. Goh LK, Sorkin A. Endocytosis of Receptor Tyrosine Kinases. *Cold Spring Harbor Perspectives in Biology* 2013;5:a017459-a017459.
26. Lacazette E, Le Calvez S, Gajendran N, Brenner HR. A novel pathway for MuSK to induce key genes in neuromuscular synapse formation. *The Journal of Cell Biology* 2003;161:727-736.
27. Moore C, Leu M, Muller U, Brenner HR. Induction of multiple signaling loops by MuSK during neuromuscular synapse formation. *Proceedings of the National Academy of Sciences* 2001;98:14655-14660.
28. Punga AR, Lin S, Oliveri F, Meinen S, Rüegg MA. Muscle-selective synaptic disassembly and reorganization in MuSK antibody positive MG mice. *Experimental Neurology* 2011;230:207-217.
29. Takata K, Stathopoulos P, Cao M, et al. Characterization of pathogenic monoclonal autoantibodies derived from muscle-specific kinase myasthenia gravis patients. *JCI Insight* 2019;4.
30. Fichtner ML, Vieni C, Redler RL, et al. Affinity maturation is required for pathogenic monovalent IgG4 autoantibody development in myasthenia gravis. *J Exp Med* 2020;217.
31. Huijbers MG, Vink AF, Niks EH, et al. Longitudinal epitope mapping in MuSK myasthenia gravis: implications for disease severity. *J Neuroimmunol* 2016;291:82-88.
32. Klooster R, Plomp JJ, Huijbers MG, et al. Muscle-specific kinase myasthenia gravis IgG4 autoantibodies cause severe neuromuscular junction dysfunction in mice. *Brain* 2012;135:1081-1101.
33. Cole RN, Reddel SW, Gervásio OL, Phillips WD. Anti-MuSK patient antibodies disrupt the mouse neuromuscular junction. *Annals of Neurology* 2008;63:782-789.
34. Chen A, Bai L, Zhong K, et al. APC2(CDH1) negatively regulates agrin signaling by promoting the ubiquitination and proteolytic degradation of DOK7. *FASEB J* 2020;34:12009-12023.
35. Otsuka K, Ito M, Ohkawara B, et al. Collagen Q and anti-MuSK autoantibody competitively suppress agrin/LRP4/MuSK signaling. *Sci Rep* 2015;5:13928.
36. Pasnoor M, Wolfe GI, Nations S, et al. Clinical findings in MuSK-antibody positive myasthenia gravis: A U.S. experience. *Muscle & Nerve* 2010;41:370-374.
37. Morsch N, Reddel SW, Ghazanfari N, Toyka KV, Phillips WD. Pyridostigmine but not 3,4-diaminopyridine exacerbates ACh receptor loss and myasthenia induced in mice by muscle-specific kinase autoantibody. *The Journal of Physiology* 2013;591:2747-2762.
38. Kawakami Y, Ito M, Hirayama M, et al. Anti-MuSK autoantibodies block binding of collagen Q to MuSK. *Neurology* 2011;77:1819-1826.

39. Witzemann V, Barg B, Criado M, Stein E, Sakmann B. Developmental regulation of five subunit specific mRNAs encoding acetylcholine receptor subtypes in rat muscle. *FEBS Letters* 1989;242:419-424.
40. Kramer C, Zoubaa S, Kretschmer A, Jordan D, Blobner M, Fink H. Denervation versus pre- and postsynaptic muscle immobilization: Effects On acetylcholine- and muscle-specific tyrosine kinase receptors. *Muscle & Nerve* 2017;55:101-108.
41. Gemza A, Barresi C, Proemer J, Hatami J, Lazaridis M, Herbst R. Internalization of Muscle-Specific Kinase Is Increased by Agrin and Independent of Kinase-Activity, Lrp4 and Dynamin. *Front Mol Neurosci* 2022;15:780659.
42. Luiskandl S, Woller B, Schlauf M, Schmid JA, Herbst R. Endosomal trafficking of the receptor tyrosine kinase MuSK proceeds via clathrin-dependent pathways, Arf6 and actin. *FEBS J* 2013;280:3281-3297.
43. Cole RN, Ghazanfari N, Ngo ST, Gervasio OL, Reddel SW, Phillips WD. Patient autoantibodies deplete postsynaptic muscle-specific kinase leading to disassembly of the ACh receptor scaffold and myasthenia gravis in mice. *J Physiol* 2010;588:3217-3229.
44. Budayeva HG, Sengupta-Ghosh A, Phu L, Moffat JG, Ayalon G, Kirkpatrick DS. Phosphoproteome Profiling of the Receptor Tyrosine Kinase MuSK Identifies Tyrosine Phosphorylation of Rab GTPases. *Mol Cell Proteomics* 2022;21:100221.

## Supplementary information

A

Clone			
13-4D3	2.1%	82.2%	15.7%
13-3D10	1.1%	97.1%	1.8%
mAb13	1.7%	97.0%	1.1%

B

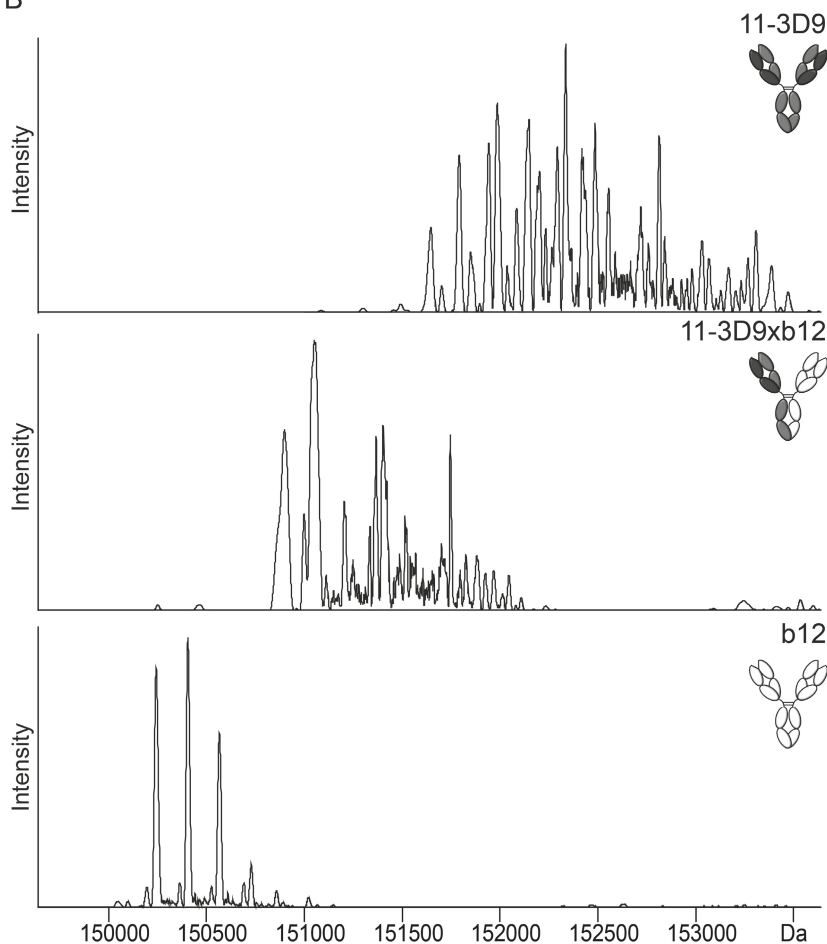
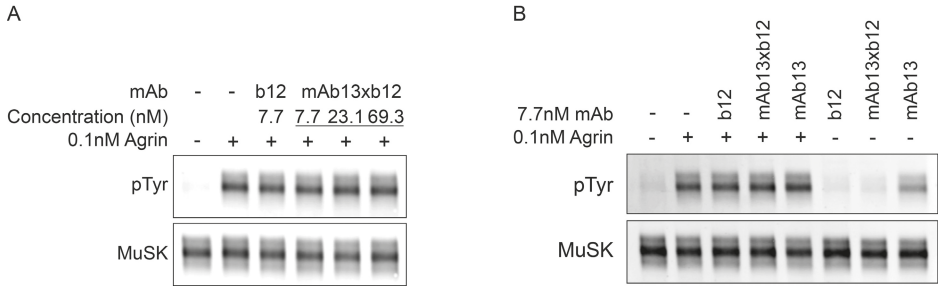
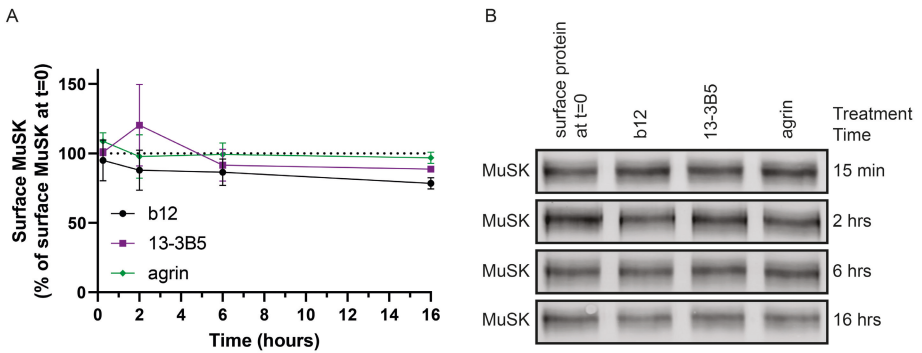


Figure S1: Exchange efficiency of monovalent MuSK antibodies. A. Relative amounts of bivalent monospecific and monovalent bispecific antibody variants after the controlled Fab-arm exchange (cFAE) reaction measured by capillary electrophoresis. B. Deconvoluted mass spectra show generation of monovalent bispecific 11-3D9xb12 after cFAE.



**Figure S2: Monovalent mAb13xb12 does not inhibit agrin-induced MuSK phosphorylation.** A. Agrin-induced MuSK phosphorylation in combination with increasing concentrations of mAb13xb12. B. MuSK phosphorylation upon addition of monovalent mAb13xb12 or bivalent mAb13 in the absence or presence of agrin.



**Figure S3: Longer exposure to agrin or bivalent 13-3B5 does not reduce surface MuSK.** A. Surface MuSK does not significantly differ over time upon exposure to agrin or bivalent 13-3B5. B. Representative blot of surface MuSK after 15 min, 2 h, 6 h or 16 h exposure. Data represent mean  $\pm$  SEM over  $n=2$  (15min, 2h and 6h) or  $n=4$  (16h) experiments.

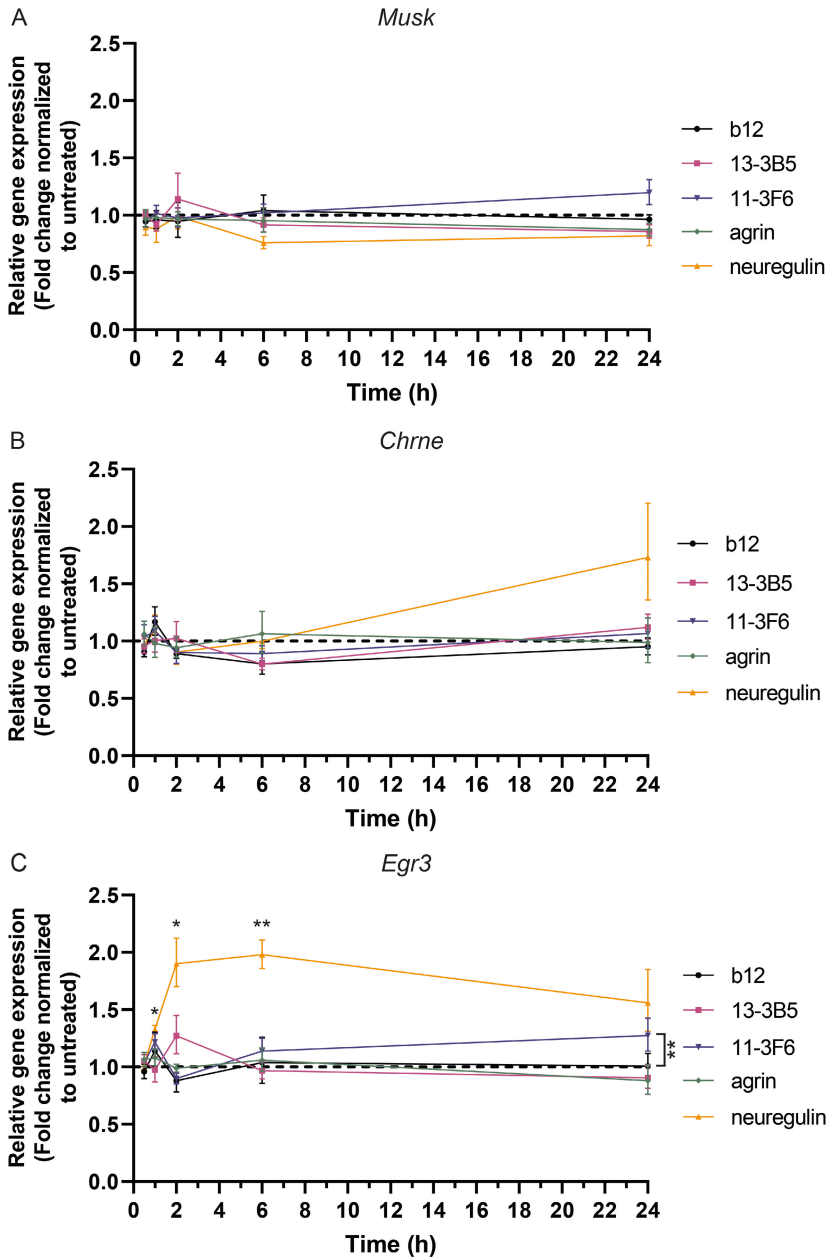


Figure S4: MuSK signalling does not directly induce gene expression of Musk or Chrne in C2C12 myotubes. Normalised gene expression of Musk (A), Chrne (B) and Egr3 (C). Egr3 expression is regulated by neuregulin and serves as a positive control for the method. 30 min ( $n=5$ ), 60 min ( $n=4$ ), 2 h ( $n=5$ ), 6 h ( $n=6$ ) and 24 h ( $n=6$ ). Data depicts geometric mean  $\pm$  geometric SEM. Paired  $t$ -test on  $\log_2$ -transformed data with Benjamini-Hochberg false discovery rate correction. \* $p < 0.05$ , \*\* $p < 0.01$ .

Table S1: Antibody conditions for western blot

Antigen	Block	Antibody buffer	Primary antibody	Secondary antibody
MuSK IP samples				
MuSK	3% BSA	Immunobooster	AF562 R&D systems 0.2µg/mL	926-32214 Licor 0.2 µg/mL
Phospho-MuSK	3% BSA	Immunobooster	05-321 Millipore 1µg/mL	926-68072 Licor 0.2 µg/mL
Dok7	3% BSA	0.5% BSA	AF6398 R&D systems 0.5µg/mL	205-032-176 Jackson ImmunoResearch 1:10.000
Whole cell lysate				
Dok7	5% milk	2% milk	AF6398 R&D systems 0.5µg/mL	205-032-176 Jackson ImmunoResearch 1:10.000
Tubulin	5% milk	2% milk	T6199 Sigma-Aldrich 0.2µg/mL	926-68072 Licor 0.2 µg/mL
Surface depletion assay				
MuSK	Odyssey Blocking Buffer	Immunobooster	AF562 R&D systems 0.2µg/mL	926-32214 Licor 0.1 µg/mL
EGFR	Odyssey Blocking Buffer	Immunobooster	51091-T52 Bioconnect 1:1000	926-32213 Licor 0.1 µg/mL
β-actin	Odyssey Blocking Buffer	Immunobooster	ab8226 Abcam 0.2µg/mL	926-68072 Licor 0.1 µg/mL

Table S2: Primers with validated amplification efficiency in C2C12 myotubes and NOD/SCID massester muscle

Gene	Accession number	Primer sequence	Amplification size (bp)	Amplification efficiency (%) C2C12	Correlation coefficient (R <sup>2</sup> ) C2C12	Amplification efficiency (%) Massester	Correlation coefficient (R <sup>2</sup> ) Massester
<i>Gapdh</i>	MGI:95640	Fw: TCCATGACAACTTTGGCATTG Rv: TCACGCCACAGCTTTCCA	103	104,3	0,998	108,8	0,996
<i>Rpl13a</i>	MGI:1351455	Fw: TGCTGCTCTCAAGGTTTGTTCC Rv: TTCTCCTCCAGAGTGGCTGT	114	98,1	1,000	104,9	0,994
<i>Egr3</i>	MGI:1306780	Fw: CTGACAATCTGTACCCCGAGGA Rv: GCTTCTCGTTGGTCAGACCCGAT	129	105,2	0,997		
<i>Musk</i>	MGI:103581	Fw: AACCCCAAACCATCTGTGTC Rv: GTCCTGCATCTCCTTTTTC	121	101,1	0,991	104,6	0,991
<i>Chrne</i>	MGI:87894	Fw: GAACCTCGTTTGAGGGTCCAG Rv: TCAGCCCAAAAGTTCACAGC	125	103,8	0,993	96,9	0,994
<i>Chrna1</i>	MGI:87885	Fw: AAGCACCTGAGGTGAAAAG Rv: CCATCACCATGGCAACATAC	118			96,6	0,992
<i>Chrn9</i>	MGI:87895	Fw: ATCGTCGTGAACCTCTGTGT Rv: CCTTCTCTCGAGCCATGAT	215			98,1	0,983
<i>Lrp4</i>	MGI:2442252	Fw: ATGGGTCTATGCGGAAAGTG Rv: CGCTCTAATTTGGCGTTCTC	121			103,4	0,991
<i>Dok7</i>	MGI:3584043	Fw: TCAGCCTCAGAAGAGCGTGTG Rv: GCCTCAGAAGAGAACTGGATAG	137			108,7	0,986
<i>Colq</i>	MGI:1338761	Fw: TGTGGTCAACAACCCAGGAAG Rv: AAAGATCGCTGGTCTCTCCG	78			100,4	0,991
<i>Ache</i>	MGI:87876	Fw: GGGCTCTACTTTCTGGTTTACG Rv: GGGCCCGGCTGATGAG	71			102,4	0,997
<i>Rapsn</i>	MGI:99422	Fw: AGGCTGGAGCCTCAAATATC Rv: AGGGCAATCTCATGGACTC	117			107,4	0,997

